Flexible, Transferable, and Thermal-Durable Dye-Sensitized Solar Cell Photoanode Consisting of TiO$_2$ Nanoparticles and Electrospun TiO$_2$/SiO$_2$ Nanofibers

Xiaoxu Wang,[†] Min Xi,[‡] Hao Fong,*[,†,‡,§] and Zhengtao Zhu*[,†,‡,§]

[†]Program of Nanoscience and Nanoengineering, [‡]Program of Materials Engineering and Science, and [§]Department of Chemistry and Applied Biological Sciences, South Dakota School of Mines and Technology, Rapid City, South Dakota 57701, United States

S *Supporting Information*

ABSTRACT: Flexible dye-sensitized solar cells (DSSCs) often face the dilemma of the high temperature sintering of TiO$_2$ photoanode to achieve superior performance and low thermal durability of the flexible substrate. Herein, we report a photoanode that combines the flexibility and high-temperature durability, which circumvents the long-standing challenge in flexible photoanode of DSSC. A hybrid mat consisting of anatase-phased TiO$_2$ nanofibers and structurally amorphous SiO$_2$ nanofibers is first prepared via the method of dual-spinneret electrospinning followed by pyrolysis. The hybrid fibrous mat is then impregnated with binder-free TiO$_2$ nanoparticles and sintered at 480 °C to form a flexible composite photoanode for DSSC. The DSSC based on this composite photoanode achieves a power conversion efficiency of 6.74 ± 0.33% on FTO/glass substrate. Device characterization and phototransient measurement, dye-loading experiment, and structural characterization indicate that, in the composite photoanode, the TiO$_2$ nanoparticles enhance the dye loading, the TiO$_2$ nanofibers improve the electron transport, and the SiO$_2$ nanofibers provide the mechanical strength/flexibility. The freestanding composite mat of TiO$_2$ nanoparticles and electrospun TiO$_2$/SiO$_2$ nanofibers, as well as the preparation methods reported herein, not only is ideal for flexible DSSCs, but also can be applied for a broad range of flexible and low-cost energy conversion devices.

KEYWORDS: dye-sensitized solar cell, flexible solar cell, electrospinning, nanofiber
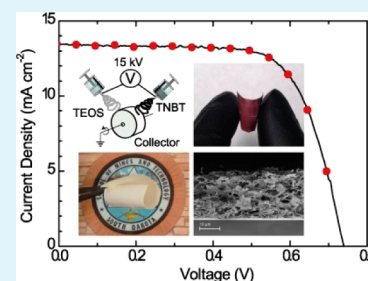
1. INTRODUCTION

Dye-sensitized solar cell (DSSC) is a promising low-cost alternative to conventional silicon solar cell owing to its high efficiency and potential low fabrication cost.[1−3] In a typical DSSC, the photoanode of mesoporous TiO$_2$ film is prepared on fluorine-doped tin oxide (FTO)/glass substrate by screen printing or doctor blading of a paste containing TiO$_2$ nanoparticles and organic binders, followed by sintering at ∼500 °C in air.[4] The photoanode is then sensitized with a monolayer of dye molecules in dark. Upon light illumination, the electrons from the photoexcited dye molecules are injected and then transport through the mesoporous TiO$_2$ film to the anode electrode. These electrons are collected at the platinum-coated counter electrode through an external load, and shuttled back to the oxidized dye molecules via redox reactions of I$^-$/I$_3^-$ redox couple in the electrolyte.

In the past decade, flexible DSSC on plastic substrate has gained great attention due to its light weight and potential low manufacturing cost via roll-to-roll (R2R) process.[5−7] The biggest challenge of flexible DSSC comes from developing photoanode suitable for plastic substrate, since sintering of TiO$_2$ mesoporous film at high temperature (∼ 500 °C) is typically required to form effective interparticle connections and to remove the organic additives in the TiO$_2$ paste. The plastic substrates cannot survive the high-temperature sintering of TiO$_2$ film, but simply lowering the sintering temperature

leads to inferior electrical properties of TiO$_2$ film.[5] The methods to solve this key issue can be broadly categorized into two approaches. In the first approach, the mesoporous TiO$_2$ film is prepared using TiO$_2$ colloid or sol−gel on flexible substrate at relatively low temperature (e.g., 150 °C).[5] In this case, the weak interparticle connection may lead to poor electron transport. Various techniques, such as mechanical compression,[8−10] hydrothermal synthesis,[11] chemical sintering,[12] and UV irradiation,[13] have been investigated to improve the interparticle connectivity. However, photoanode sintered at low temperature still bears large inherent resistance and short electron lifetime and needs further investigation in order to improve the electron transport and the efficiency of the flexible DSSC. Additionally, photoanode sintered at low temperature typically requires paste of TiO$_2$ nanoparticles without organic binder, and the formation of cracks in the photoanode film during the solvent evaporation is often a serious issue. The other approach to flexible photoanode is to prepare mesoporous TiO$_2$ film at high temperature (e.g., 500 °C) directly on flexible metal foil substrate or to develop a process to transfer the TiO$_2$ film sintered at high temperature to plastic substrate.[14−20] Photoanode of mesoporous TiO$_2$ film prepared

by this approach may achieve superior DSSC performance similar to that of the photoanode in conventional DSSC on FTO/glass substrate. However, flexible DSSC using metal foil as substrate requires illumination from the counter electrode side, which may lead to significant photon loss due to the absorption of electrolyte and catalyst on the counter electrode.[14−16] Additionally, the high cost and corrosion-related issues of metal substrate may limit its application in flexible DSSC.[5] Transfer of the TiO$_2$ film sintered at high temperature to plastic substrate has the advantages of high temperature sintering and front-side (i.e., photoanode side) illumination through the flexible substrate.[17,19,20] The major drawback of the transfer approach is that the mesoporous film of TiO$_2$ nanoparticles becomes very fragile after sintering, which makes it nearly impossible to prepare large-area photoanode on flexible substrate. Therefore, a flexible, scalable, low-cost, and thermal-durable photoanode material is in demand for fabricating flexible DSSC with high efficiency.

Electrospinning is a facile, low-cost, and scalable technique for preparing one-dimensional (1-D) nanomaterials including polymer, ceramic, and carbon/graphite fibers with diameters typically ranging from tens to hundreds of nanometers.[21] Electrospun TiO$_2$ nanostructures have been investigated as photoanode materials in DSSC.[22−24] Previous studies have demonstrated that incorporation of 1-D TiO$_2$ nanostructures into DSSC photoanode can improve the overall device efficiency through increasing the electron lifetime.[22−31] The typical TiO$_2$ nanofibers prepared by electrospinning are polycrystalline and mechanically fragile. Such electrospun TiO$_2$ nanostructures are not suitable for flexible DSSCs. Electrospun polymer nanofibers have been studied as scaffold for incorporating binder-free TiO$_2$ nanoparticles as a flexible photoanode on plastic substrate.[32] The polymer nanofibrous mat/film greatly improves the bendability of TiO$_2$ photoanode by relieving the external stress and preventing crack generation and propagation in the film. The trade-off is the efficiency of DSSC cell due to the increased cell impedance upon incorporation of polymer nanofibers in the photoanode.

In this paper, we report a transferable, thermal-durable, and freestanding DSSC photoanode mat of metal oxides prepared by electrospinning. By incorporating ∼25 wt % amorphous SiO$_2$ nanofibers within the TiO$_2$ nanofibrous mat via a dual-spinneret electrospinning method followed by pyrolysis at high temperature, we have successfully prepared a hybrid mat of TiO$_2$/SiO$_2$ nanofibers (denoted as TS-Mat) with superior mechanical strength and flexibility. Binder-free TiO$_2$ nanoparticles have subsequently been impregnated into the hybrid mat followed by sintering at 480 °C to form the resulting DSSC photoanode consisting of TiO$_2$ nanoparticles and the hybrid mat (denoted as TS-Mat-NP). DSSCs containing the photoanodes of the composite mat TS-Mat-NP on both FTO/glass and indium tin oxide (ITO)/polyethylene terephthalate (PET) substrates have been fabricated and characterized. It is envisioned that the freestanding and high-temperature-durable composite mat of TS-Mat-NP prepared by scalable electrospinning technique has the potential for future large-area, low-cost, and flexible photovoltaic and other energy conversion applications.

2. EXPERIMENTAL SECTION

2.1. Materials. Titanium(IV) butoxide (TNBT), titanium(IV) isopropoxide (TTIP), tetraethyl orthosilicate (TEOS), polyvinylpyrrolidone (PVP, Mw = 1 300 000), indium tin oxide coated PET film

(ITO/PET, 60 Ω/sq), and all solvents were purchased from Sigma-Aldrich Chemical Co. The F-doped SnO$_2$ glass (FTO/glass, 8 Ω/sq) was provided by Hartford Glass Co. The dye cis-diisothiocyanato-bis(2,2′-bipyridyl-4,4′-dicarboxylato) ruthenium(II) bis-(tetrabutylammonium) (N719), the platinum precursor (Platisol T), and the electrolyte (Iodolyte AN-50) were acquired from Solaronix (Switzerland). All chemicals were used as received without further purification.

2.2. Preparation and Characterization of Hybrid Mat Consisting of TiO$_2$/SiO$_2$ and TiO$_2$ Nanoparticles. The hybrid nanofibrous mat of TiO$_2$/SiO$_2$ was prepared using the dual-spinneret electrospinning technique, as reported in our previous publication.[33] In brief, the TNBT spin dope was prepared by mixing a solution of 3 g of TNBT in 1.5 g of HAc/H$_2$O with another solution of 1.1 g of PVP in 4.9 g of IPA and 8.2 g of DMF. The TEOS spin dope was prepared by mixing a solution of 1.5 g of TEOS in 0.6 g of HCl aqueous solution and 0.4 g of ethanol with another solution of 1.1 g of PVP in 4.9 g of IPA and 8.2 g of DMF. The two syringes containing TNBT or TEOS spin dope were placed horizontally at the opposite sides of a grounded rotating roller collector. The flow rates for the TNBT and TEOS spin dopes were set at 1.84 and 0.60 mL/h, respectively. During the electrospinning process, a DC voltage of 15 kV was applied to the metallic needles of both spinnerets, and the nanofibers were collected on an aluminum foil covering the roller collector. The as-spun nanofibrous mat on the aluminum foil was kept in air for 48 h to allow for complete hydrolysis of TNBT and TEOS precursors; thereafter, the mat was sintered at 500 °C for 10 h at the ramping rate of 1 °C/min in a tube furnace with constant air flow. When the TNBT spinneret was removed from the system and other parameters were maintained, the neat SiO$_2$ nanofibrous mat was readily prepared.

The synthesis of TiO$_2$ nanoparticles followed a modified procedure reported elsewhere.[34] In brief, 1.25 g of TTIP was first diluted with 1.25 g of IPA. The solution was then added dropwise to a 20-mL vial containing 2 mL of acetic acid (99%, 17.4 M) and 8 mL of deionized water with vigorous stirring. The vial was then transferred to a 90 °C water bath with continuous stirring. The solvent was slowly evaporated during the reaction, and the heat was removed until a TiO$_2$ concentration of 14 wt % was reached. The product was a translucent gel, and was ready to use as binder-free paste of TiO$_2$ nanoparticles for doctor blading.

The morphologies of the hybrid mats and the TiO$_2$ nanoparticles paste were characterized by a Zeiss Supra 40VP field-emission scanning electron microscope (SEM) equipped with an Oxford AZtecEnergy advanced system for energy-dispersive X-ray micro-analysis (EDS or EDX), and a JEOL JEM-2100 high-resolution transmission electron microscope (HRTEM). The BET surface area was determined by a Micromeritics Chmisorb 2720 Pulse Chemisorption System.

2.3. DSSC Fabrication. ITO/PET and FTO/glass substrates were cleaned in a sequence of detergent solution, deionized water, acetone, and isopropanol for 15 min each under sonication. To prepare the photoanode, the binder-free paste of TiO$_2$ nanoparticles was applied onto the surface of the ITO/PET or FTO/glass by doctor blading, followed by placing a piece of hybrid mat on the TiO$_2$ nanoparticles layer. Then, a moderate pressure of ∼0.3 MPa was used to squeeze the TiO$_2$ paste into the hybrid mat. Finally, the photoanode on ITO/PET was obtained after the sample was heated at 150 °C for 2 h; the photoanode on FTO/glass was obtained after the sample was sintered at 480 °C for 1 h. The photoanode was sensitized by immersing it in a 0.3 mM N719 dye in ethanol solution for 18 h at room temperature. The counter electrode was prepared by annealing platinum precursor Platisol T on a FTO/glass substrate with two drilled holes at 385 °C for 15 min. The photoanode and the counter electrode were sealed together using parafilm at 100 °C, followed by injection of the Iodolyte AN-50 electrolyte through the drilled holes on the counter electrode glass. Finally, the drilled holes were sealed using parafilm. Three identical cells were fabricated for each type of DSSC device.

2.4. Photovoltaic Characterization and Transient Photovoltage Measurement. The solar cell performance was characterized using a Keithley 2400 sourcemeter. A 150-W Solar Simulator

(Newport Co.) was used to simulate 100 mW cm^{-2} sunlight. The light intensity was adjusted using a Hamamatsu S1133 reference cell calibrated by the National Renewable Energy Laboratory.

The electron recombination lifetime (τ_e) was measured using a transient photovoltage setup as reported previously.[23] In brief, under open-circuit condition, a white-light-emitting diode (LED) array was used to establish a bias open-circuit photovoltage of the device. A red LED pulse with 200-μs pulse width was shined on the cell to give a small rise of the photovoltage. The decay of such photovoltage perturbation was recorded via an oscilloscope. The recombination lifetime of electron under specified bias light intensity was obtained by fitting the decay curve with single exponential decay function.

3. RESULTS AND DISCUSSION

3.1. Preparation of TS-Mat-NP and Assembly of DSSC Photoanode.
We recently developed a facile electrospinning approach to prepare hybrid mats containing two or more types of nanofibers.[33] Figure 1a shows the scheme of preparing a
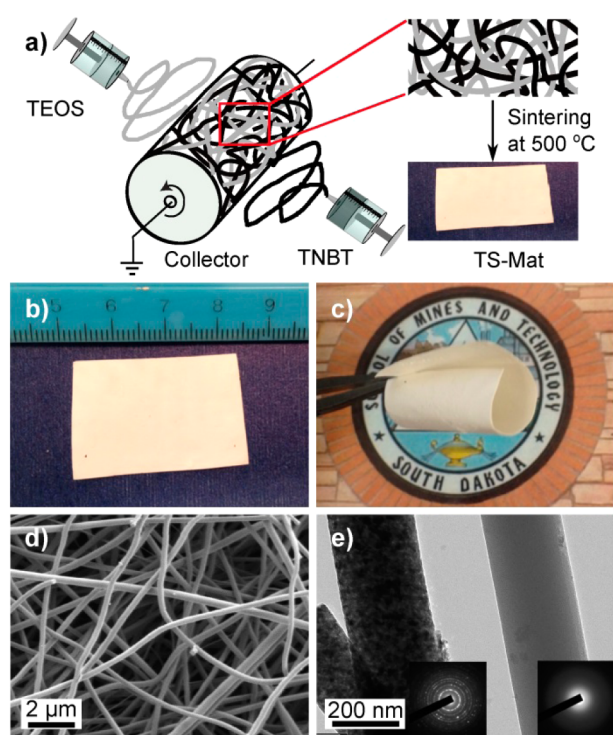

Figure 1. (a) Schematic showing the preparation of hybrid mat of TiO$_2$/SiO$_2$ nanofibers (TS-Mat) via dual-spinneret electrospinning technique, (b) and (c) optical images of TS-Mat, (d) SEM image of TS-Mat, (e) TEM image of TiO$_2$ nanofiber and SiO$_2$ nanofiber in TS-Mat. The insets: SAED patterns showing anatase structure of TiO$_2$ (left) and amorphous structure of SiO$_2$ (right).

hybrid mat of TiO$_2$/SiO$_2$ nanofibers via the dual-spinneret electrospinning approach. The TiO$_2$ precursor (TNBT) nanofibers and the SiO$_2$ precursor (TEOS) nanofibers with desired ratio were electrospun simultaneously by controlling compositions and flow rates of spin dopes. After post-electrospinning hydrolysis and sintering, the freestanding and mechanically flexible hybrid mat of TiO$_2$/SiO$_2$ (TS-Mat in Figure 1a) was formed. On the basis of the flow rates and the contents of the spin dopes, we estimated that the hybrid nanofibrous mat of TiO$_2$/SiO$_2$ consisted of ~75 wt % TiO$_2$ nanofibers and ~25 wt % SiO$_2$ nanofibers. The EDS results (Figure S1 and Table S1 in Supporting Information (SI)) further confirmed the composition of hybrid nanofibrous mat

of TiO$_2$/SiO$_2$. Using the setup, a large-area hybrid mat of TiO$_2$/SiO$_2$ nanofibers was readily made, as shown in Figure 1b for a 3 cm × 2 cm hybrid mat. The typical thickness of the TS-Mat is ~30 μm. Figure 1c shows that the freestanding TiO$_2$/SiO$_2$ mat was wrapped into cylindrical form, demonstrating the excellent bendability and flexibility of the material. More images of the hybrid mat under bending condition are shown in Figure S2 (SI). The SEM image in Figure 1d depicts that the hybrid mat contained the intertwined TiO$_2$ nanofibers and SiO$_2$ nanofibers with diameters from 200 to 600 nm. All nanofibers in the mat had smooth surface, and the TiO$_2$ nanofibers and SiO$_2$ nanofibers were not distinguishable in the SEM image. The structure and morphology of the hybrid mat was further examined with TEM. As shown in Figure 1e, the TiO$_2$ nanofiber was composed of well-connected polycrystalline crystallites/grains with sizes of ~10−20 nm, while the SiO$_2$ nanofibers contained no gains or lattice fringes. The selected-area electron diffraction (SAED) patterns (insets of Figure 1e) confirmed that the TiO$_2$ nanofibers had anatase crystalline structure and the SiO$_2$ nanofibers were structurally amorphous. We believe that the amorphous SiO$_2$ nanofibers are essential for the flexibility of hybrid mat of TiO$_2$ and SiO$_2$. It is known that the polycrystalline TiO$_2$ nanofibrous mat (or film) is mechanically fragile, and only the mat with relatively small size could be obtained.[35] Figure S3 (SI) shows the comparison between the neat TiO$_2$ nanofibrous mat and the TiO$_2$/SiO$_2$ hybrid nanofibrous mat under bending. Clearly, the neat TiO$_2$ nanofibrous mat was broken after bending, whereas the hybrid mat of TiO$_2$/SiO$_2$ nanofibers was still intact. The inclusion of structurally amorphous SiO$_2$ nanofibers not only facilitates the stress release during bending,[32,36] but also serves as spacers to reduce the conglutination points between fragile TiO$_2$ nanofibers.[33]

The relatively open nanofibrous network as shown in Figure 1d may be ideal for releasing the stress during bending and as a template for incorporation of other functional materials. Figure 2 shows the impregnation of binder-free TiO$_2$ nanoparticles in hybrid mat of TiO$_2$/SiO$_2$ nanofibers to form a composite mat consisting of TiO$_2$/SiO$_2$ nanofibers and TiO$_2$ nanoparticles (denoted as TS-Mat-NP) for photoanode in DSSC. The TEM images of the TiO$_2$ nanoparticles and the composite mat are shown in Figure S4 (SI). The freestanding hybrid mat of TiO$_2$/SiO$_2$ nanofibers was pressed on the TiO$_2$ nanoparticle layer right after the layer was prepared by doctor-blading of binder-free TiO$_2$ nanoparticles paste. During the process, the TiO$_2$ nanoparticles were squeezed into the hybrid nanofibrous mat of TiO$_2$/SiO$_2$. After sintering at 150 °C, a flexible and bendable photoanode on the ITO/PET film (denoted as TS-Mat-NP/ITO) was prepared. The photoanode of the composite mat on the FTO/glass substrate (denoted as TS-Mat-NP/FTO) was made by sintering at 480 °C for 1 h. It is noteworthy that the binder-free paste of TiO$_2$ nanoparticles alone formed cracks and flaked off from the substrate after doctor blading and solvent evaporation, and was not possible to be used as photoanode film (Figure S5a−c, SI). On the other hand, as shown in Figure S5 d−f, the photoanode composed of TiO$_2$/SiO$_2$ nanofibers and TiO$_2$ nanoparticles (i.e., TS-Mat-NP) was still crack-free and mechanically intact even after 300 bending cycles. The network of TiO$_2$ and SiO$_2$ nanofibers helped relieve the surface tension during solvent evaporation, and led to crack-free and mechanically robust/flexible photoanode.[32]

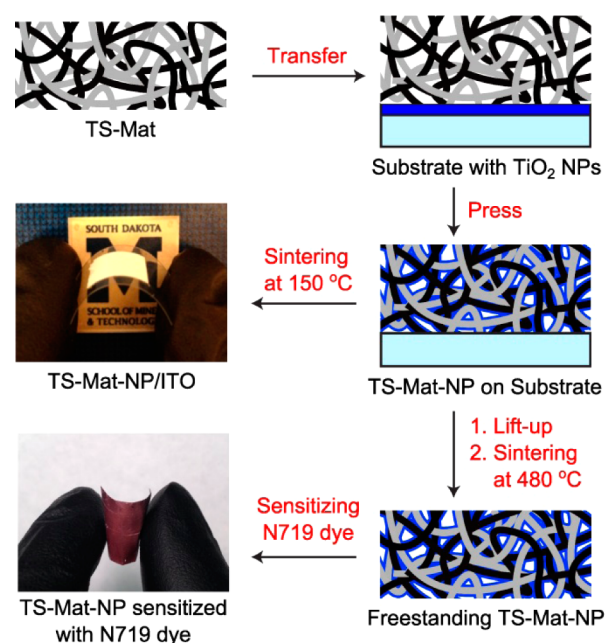The superior mechanical strength and flexibility of the hybrid nanofibrous mat of TiO$_2$/SiO$_2$ enabled us to process the

Figure 2. Schematic showing fabrication of freestanding composite mat (TS-Mat-NP) containing hybrid nanofibrous TiO_2/SiO_2 mat (TS-Mat) and bind-free TiO_2 nanoparticles (NPs) (top), photoanode of TS-Mat-NP sintered at 150 °C on ITO/PET substrate (denoted as TS-Mat-NP/ITO) (middle), and freestanding TS-Mat-NP sintered at 480 °C followed by sensitization of N719 dye (bottom).

freestanding hybrid mat without the support of a substrate. For example, a freestanding composite mat containing TiO_2/SiO_2 nanofibers and TiO_2 nanoparticles was readily prepared by doctor-blading the paste of TiO_2 nanoparticles on the hybrid nanofibrous mat directly. In this work, a lift-up method was used to detach the composite mat from ITO/PET substrate (Figure 2).[17] The composite mat after lift-up was sintered at 480 °C, and then sensitized with N719 dye. The freestanding photoanode of TS-Mat-NP (as shown in Figure 2) after sintering at 480 °C and sensitization in N719 solution retained its superior flexibility and bendability. The SEM images of the TS-Mat-NP photoanode on FTO/glass substrate (TS-Mat-NP/FTO) are shown in Figure S6 (SI). In TS-Mat-NP/FTO, TiO_2 nanoparticles clusters were attached on TiO_2/SiO_2 nanofibers, and dispersed evenly throughout the TS-Mat-NP photoanode. The nanoparticles and nanofibers are bonded together after sintering to form a thermal-durable and stable composite mat. It is likely that Ti−O−Ti or Ti−O−Si bonds are formed between nanoparticles and nanofibers due to the condensation of −OH groups on the surface of nanoparticles and nanofibers during the sintering process.[34] The thickness of the TS-Mat-NP photoanode was ~23 μm, less than the thickness of the TS-Mat due to the applied pressure during impregnation of TiO_2 nanoparticles.

It is known that electrospun TiO_2 nanofibers have relatively low specific surface area, which limits their application in DSSC.[31] The dye desorption experiment (see experimental details in SI) indicated that the dye loading of the hybrid mat of TiO_2/SiO_2 (TS-Mat), the composite mat on ITO/PET (TS-Mat-NP/ITO), and the composite mat on FTO/glass (TS-Mat-NP/FTO) were 9.90×10^{-9}, 1.32×10^{-7}, and 1.36×10^{-7} mol cm^{-2}, respectively. The dye loading after impregnation of TiO_2 nanoparticles was similar to that of photoanode based on P25 TiO_2 nanoparticles,[24] which was more than 1 order of

magnitude higher than the dye loading of hybrid nanofibrous mat of TiO_2/SiO_2. The BET surface area of TS-Mat-NP was measured to be 166 m^2 g^{-1}, which was much higher than that of the TS-Mat (typically in the range from ~10 to 25 m^2 g^{-1}).[31] Clearly, the binder-free TiO_2 nanoparticles in the composite mat TS-Mat-NP increased the surface area of the hybrid nanofibrous mat of TiO_2/SiO_2, and subsequently improved the dye adsorption.

3.2. Photovoltaic Performance. We have evaluated the performance of the DSSCs based on the photoanode consisting of electrospun TiO_2/SiO_2 nanofibers and TiO_2 nanoparticles. The device based on the composite mat of neat SiO_2 nanofibers/TiO_2 nanoparticles was used as comparison. The composite mats of SiO_2 nanofibers/TiO_2 nanoparticles (denoted as S-Mat-NP) were prepared following the same procedure outlined in Figure 2. Four types of photoanodes were used in DSSC devices: composite mats of TiO_2/SiO_2 nanofibers and TiO_2 nanoparticles sintered at 150 °C for 2 h on ITO/PET film (TS-Mat-NP/ITO) or sintered at 480 °C for 1 h on FTO/glass (TS-Mat-NP/FTO), composite mats of neat SiO_2 nanofibers/TiO_2 nanoparticles sintered at 150 °C for 2 h on ITO/PET (S-Mat-NP/ITO) or sintered at 480 °C for 1 h on FTO/glass (S-Mat-NP/FTO). The optical images of the devices are shown in Figure S7 (SI). All devices were assembled in one batch, and three identical cells were fabricated for each type of device. The average of the solar cell parameters of the three identical cells and the standard deviation were calculated and are summarized in Table 1. The J−V curves of the DSSCs are shown in Figure 3.

Table 1. Photovoltaic Parameters of the DSSCs Based on Different Photoanodes

sample[a]	η (%)	j_{sc} (ma cm^{-2})	V_{oc} (mV)	FF (%)
TS-Mat-NP/FTO	6.74 ± 0.33	13.2 ± 0.70	740 ± 0	69.4 ± 0.3
S-Mat-NP/FTO	3.98 ± 0.56	7.45 ± 1.02	748 ± 3	71.5 ± 0.8
TS-Mat-NP/ITO	1.06 ± 0.06	2.72 ± 0.11	637 ± 6	61.3 ± 0.5
S-Mat-NP/ITO	0.40 ± 0.03	1.09 ± 0.08	590 ± 4	62.1 ± 0.2

[a]TS-Mat-NP/FTO: composite of hybrid nanofibrous TiO_2/SiO_2 mat and TiO_2 nanoparticles on FTO/glass substrate; S-Mat-NP/FTO: composite of SiO_2 nanofibrous mat and TiO_2 nanoparticles on FTO/glass substrate; TS-Mat-NP/ITO: composite of hybrid nanofibrous TiO_2/SiO_2 mat and TiO_2 nanoparticles on ITO/PET substrate; S-Mat-NP/ITO: composite of SiO_2 nanofibrous mat and TiO_2 nanoparticles on ITO/PET substrate.

The DSSC based on the composite of nanofibrous mat of TiO_2/SiO_2 and TiO_2 nanoparticles on the FTO/glass substrate (TS-Mat-NP/FTO) exhibited the efficiency of 6.74 ± 0.33%, ~70% higher than that of the DSSC based on composite of neat SiO_2 nanofibrous mat/TiO_2 nanoparticles (S-Mat-NP/FTO). The enhanced efficiency was largely from the significantly higher short-circuit current density (J_{sc}) of photoanode of TS-Mat-NP/FTO (13.2 ± 0.7 mA cm^{-2}) than that of photoanode of S-Mat-NP/FTO (7.45 ± 1.02 mA cm^{-2}). There was no appreciable difference between the open-circuit voltage (V_{oc}) and the fill factor (FF) of both devices. Both devices were prepared under the same condition, and the only difference between the two devices was the presence of TiO_2 nanofibers in the device based on photoanode of TS-Mat-NP/FTO. Therefore, the improved DSSC performance could be attributed to the presence of TiO_2 nanofibers in the composite
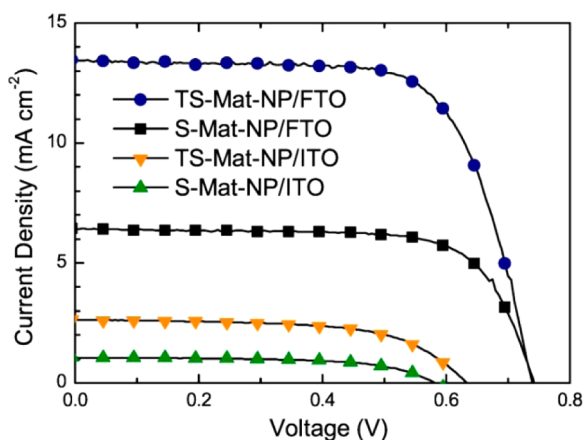
Figure 3. $J-V$ characteristics of DSSCs based on the composite photoanodes of nanofibrous mat and TiO_2 nanoparticles on FTO/glass or ITO/PET substrates. TS-Mat-NP/FTO: composite of hybrid nanofibrous TiO_2/SiO_2 mat and TiO_2 nanoparticles on FTO/glass substrate; S-Mat-NP/FTO: composite of SiO_2 nanofibrous mat and TiO_2 nanoparticles on FTO/glass substrate; TS-Mat-NP/ITO: composite of hybrid nanofibrous TiO_2/SiO_2 mat and TiO_2 nanoparticles on ITO/PET substrate; S-Mat-NP/ITO: composite of SiO_2 nanofibrous mat and TiO_2 nanoparticles on ITO/PET substrate.

photoanode. When the photoanodes were fabricated on the ITO/PET substrate at 150 °C, the DSSC based on composite photoanode of TiO_2/SiO_2 nanofibrous mat and TiO_2 nanoparticles (TS-Mat-NP/ITO) had an efficiency of $1.06 \pm 0.06\%$, with J_{sc} of 2.72 ± 0.11 mA cm^{-2}, V_{oc} of 637 ± 6 mV, and FF of $61.3 \pm 0.5\%$; the DSSC based on composite photoanode of neat SiO_2 nanofibrous mat and TiO_2 nanoparticles (S-Mat-NP/ITO) had an efficiency of $0.40 \pm 0.03\%$, with J_{sc} of 1.09 ± 0.08 mA cm^{-2}, V_{oc} of 590 ± 4 mV, and FF of $62.1 \pm 0.2\%$. Compared with the device based on S-Mat-NP/ITO, the cell based on TS-Mat-NP/ITO containing TiO_2 nanofibers had 165% higher efficiency, 150% higher J_{sc}, and 8% higher V_{oc}; there was a slight difference between the FF values of the two devices. The results indicated that the presence of TiO_2 nanofibers in TS-Mat-NP/ITO was essential to improve the device efficiency.

In general, the efficiency of DSSC is determined by three factors: light harvesting efficiency (η_{lh}), electron injection efficiency (η_{inj}), and electron collection efficiency (η_{col}). J_{sc} is the integration of η_{lh}, η_{inj}, η_{col} and the spectral photon flux of the light source over the dye absorption range.[37] η_{inj} is expected to be very similar in all four devices.[37] η_{lh} depends linearly on the amount of dye molecules attached on the TiO_2 mesoporous film.[38,39] The dye loading of TS-Mat-NP which was impregnated with TiO_2 nanoparticles (1.36×10^{-7} mol cm^{-2}) was more than an order of magnitude higher than the dye loading of nanofibrous mat TS-Mat (9.90×10^{-9} mol cm^{-2}), suggesting that the dye loading was largely determined by the amount of TiO_2 nanoparticles. Hence, the dye loading of four devices in Table 1 would be similar, leading to similar η_{lh} for all four devices. The increase of J_{sc} in devices with TiO_2 nanofibers in the photoanode (TS-Mat-NP/FTO and TS-Mat-NP/ITO) was likely due to the improved η_{col} through suppressing electron recombination. This was in line with our previous studies on the composite films of TiO_2 nanofibers and nanoparticles as DSSC photoanode, in which we concluded that the one-dimensional TiO_2 nanofibers can suppress electron recombination and enhance η_{col}.[22,23]

To understand the electron recombination behavior within the DSSCs, we extract the electron recombination lifetime (τ_e) using the transient photovoltage measurement. The electron recombination depends on the incident light intensity, and more specifically, on the quasi-Fermi level within the TiO_2 band gap under illumination.[39] Because V_{oc} is determined by the difference between the quasi-Fermi level under illumination and the energy level of the redox couple,[40] the logarithm of τ_e as a function of V_{oc} is shown in Figure 4.
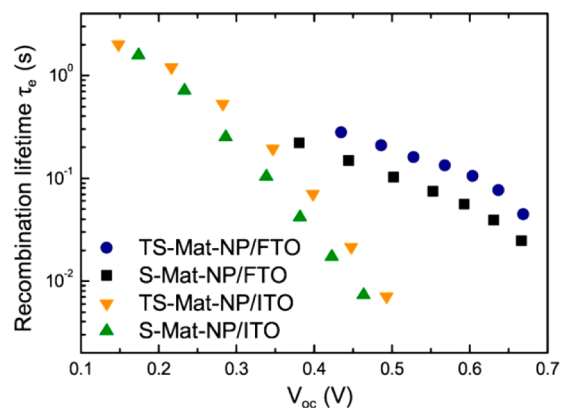

Figure 4. Electron recombination lifetime (τ_e) as a function of open-circuit voltage (V_{oc}). TS-Mat-NP/FTO: composite of hybrid nanofibrous TiO_2/SiO_2 mat and TiO_2 nanoparticles on FTO/glass substrate; S-Mat-NP/FTO: composite of SiO_2 nanofibrous mat and TiO_2 nanoparticles on FTO/glass substrate; TS-Mat-NP/ITO: composite of hybrid nanofibrous TiO_2/SiO_2 mat and TiO_2 nanoparticles on ITO/PET substrate; S-Mat-NP/ITO: composite of SiO_2 nanofibrous mat and TiO_2 nanoparticles on ITO/PET substrate.

Generally, the electron lifetimes of all four devices decrease with the increase of light intensity. The electron lifetimes of devices containing TiO_2 nanofibers (TS-Mat-NP/FTO and TS-Mat-NP/ITO) are much longer than those of devices without TiO_2 nanofibers (S-Mat-NP/FTO and S-Mat-NP/ITO), indicating that the electron recombination is reduced in the photoanodes containing TiO_2 nanofibers. The increase of electron lifetime leads to the observed improvement of cell performance in the photoanodes of the composite of the hybrid TiO_2/SiO_2 nanofibrious mat and TiO_2 nanoparticles, compared to the photoanodes with neat SiO_2 nanofibers and TiO_2 nanoparticles.

3.3. Effect of the Sintering Temperature. The devices on the ITO/PET substrate, sintered at 150 °C, had considerably lower efficiency than the devices on the FTO/glass, sintered at 480 °C (Table 1). According to the literature, DSSCs with ITO electrode instead of FTO electrode may have slightly lower J_{sc} and FF, due to the lower light transmittance and less conductivity of ITO electrode.[14,41] Thus, the observed efficiency difference in our devices on FTO/glass and ITO/PET substrates (Table 1) was likely due to the effect of sintering temperature,[42,43] since other fabrication conditions were identical. Figure 5 depicts the dependence of η, J_{sc}, V_{oc}, and FF on the sintering temperature for DSSCs based on composite photoanode of hybrid TiO_2/SiO_2 nanofibrous mat and TiO_2 nanoparticles on FTO/glass substrate. It is evident that the efficiency η and the J_{sc} increased almost linearly with the rise of sintering temperature. The V_{oc} decreased slightly initially and then gained a noticeable increase with the increase of temperature. The FF was much improved when the sintering
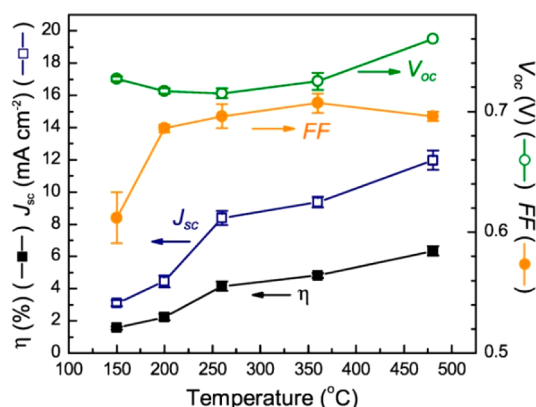
Figure 5. Dependence of conversion efficiency (η), short-circuit photocurrent density (J_{sc}), open-circuit voltage (V_{oc}), and fill factor (FF) on the sintering temperature.

temperature increased from 150 to 200 °C, then the change of FF was relatively small from 200 to 480 °C.

It is noteworthy that the improvement of efficiency strongly correlates with J_{sc}. As we have discussed previously, the J_{sc} is mainly influenced by the collection efficiency of electrons, and more specifically, by the recombination loss of electrons. As shown in Figure 4, the recombination lifetimes of DSSCs on ITO/PET substrate (TS-Mat-NP/ITO and S-Mat-NP/ITO) were much shorter at the same V_{oc} and decreased much faster than those of DSSCs on FTO/glass substrate (TS-Mat-NP/ITO and S-Mat-NP/ITO). If we extrapolated the data to the V_{oc} under AM 1.5 illumination, the recombination lifetimes of devices on ITO/PET substrate were estimated to be an order of magnitude shorter than those of devices on FTO/glass substrate. Therefore, the improvement of J_{sc} at high temperature could be attributed to the reduced electron recombination with the increase of sintering temperature.

The increase of efficiency with increasing of sintering temperature during preparation of photoanode in DSSC is generally attributed to the improved connection between TiO$_2$ nanoparticles.[42,43] The effect of sintering temperature on the composite photoanode of TiO$_2$ nanoparticles and TiO$_2$/SiO$_2$ nanofibers was further investigated using TEM and SEM to compare the morphologies of the photoanodes sintered at low temperature and at high temperature (see SI). From the SEM and TEM images in Figure S8 (SI), it is clear that the grain size of TiO$_2$ nanoparticles increased after high temperature sintering, confirming that the high temperature sintering improved the interparticle connection. As a consequence, the electron collection efficiency was improved in the composite photoanode sintered at higher temperature, leading to enhanced J_{sc} and the device efficiency.

4. CONCLUSIONS

A freestanding and flexible hybrid mat consisting of 75 wt % anatase-phased TiO$_2$ nanofibers and 25 wt % amorphous SiO$_2$ nanofibers was prepared via the dual-spinneret electrospinning method. TiO$_2$ nanoparticles were impregnated into the hybrid nanofibrous mat to form a composite mat, which was used as photoanode in DSSCs on both ITO/PET and FTO/glass substrates. The $J-V$ characteristic and the transient photo-voltage characterization results indicated that the TiO$_2$ nanofibers within composite photoanode could significantly improve the device efficiency through suppressing recombina-

tion. The performance of the devices based on composite photoanodes sintered at different temperatures revealed that the high temperature sintering improved the interparticle connection and reduced recombination, resulting in the enhanced J_{sc} and device efficiency. The device based on the composite photoanode of hybrid nanofibrous TiO$_2$/SiO$_2$ mat and TiO$_2$ nanoparticles achieved conversion efficiency of 6.74 ± 0.33% on FTO/glass substrate. Additionally, the flexible composite of hybrid nanofibrous TiO$_2$/SiO$_2$ mat and TiO$_2$ nanoparticles retained superior flexibility and integrality after sintered at 480 °C, and was further processed as a free-standing photoanode for dye sensitization.

In summary, the composite of hybrid nanofibrous TiO$_2$/SiO$_2$ mat and TiO$_2$ nanoparticles is flexible and bendable; and, more importantly, the material can be processed at high temperature as a freestanding film and serve as photoanode of DSSC with high efficiency. We can envision a substrate-free flexible DSSC using dye-sensitized freestanding photoanode of TiO$_2$/SiO$_2$ nanofibers and TiO$_2$ nanoparticles (such as TS-Mat-NP in Figure 2), solid electrolyte, and transparent conducting electrodes deposited directly on the composite mat.[17,44,45] Roll-to-roll (R2R) processes may be developed to fabricate such a substrate-free DSSC. Work along this direction is underway.

■ ASSOCIATED CONTENT

Ⓢ Supporting Information

Energy-dispersive X-ray spectrum of the hybrid nanofibrous mat of TiO$_2$/SiO$_2$; optical images of hybrid nanofibrous mat of TiO$_2$/SiO$_2$; optical images of the bending test of the neat TiO$_2$ nanofibrous mat and the hybrid TiO$_2$/SiO$_2$ nanofibrous mat; TEM images of TiO$_2$ nanoparticles and TiO$_2$/SiO$_2$ nanofibers; optical images of preparation of photoanode film based on binder-free TiO$_2$ nanoparticles and the bending test of the hybrid mat on PET substrate; SEM images of the composite of hybrid nanofibrous mat and TiO$_2$ nanoparticles on FTO substrate or the freestanding composite mat; optical images of four devices; SEM images of the composite photoanode of hybrid nanofibrous TiO$_2$/SiO$_2$ mat and TiO$_2$ nanoparticles sintered at 150 or 480 °C; detailed discussion on the effect of sintering temperature; procedure for dye loading measurement. This material is available free of charge via the Internet at http://pubs.acs.org.

■ AUTHOR INFORMATION

Corresponding Authors

*Tel.: 605-394-1229. Fax: 605-394-1232. E-mail: Hao.Fong@sdsmt.edu.

*Tel.: 605-394-2447. Fax: 605-394-1232. E-mail: Zhengtao.Zhu@sdsmt.edu.

Author Contributions

The manuscript was written through contributions of all authors. All authors have given approval to the final version of the manuscript.

Notes

The authors declare no competing financial interest.

■ REFERENCES

(1) O'Regan, B.; Grätzel, M. A Low-Cost, High-Efficiency Solar Cell Based on Dye-Sensitized Colloidal TiO_2 Films. *Nature* **1991**, *353*, 737−740.

(2) Mathew, S.; Yella, A.; Gao, P.; Humphry-Baker, R.; Curchod, B. F. E.; Ashari-Astani, N.; Tavernelli, I.; Rothlisberger, U.; Nazeeruddin, Md. K.; Grätzel, M. Dye-Sensitized Solar Cells with 13% Efficiency Achieved Through the Molecular Engineering of Porphyrin Sensitizers. *Nat. Chem.* **2014**, *6*, 242−247.

(3) Upadhyaya, H. M.; Senthilarasu, S.; Hsu, M.-H.; Kumar, D. K. Recent Progress and the Status of Dye-Sensitized Solar Cell (DSSC) Technology with State-of-the-Art Conversion Efficiencies. *Sol. Energy Mater. Sol. Cells* **2013**, *119*, 291−295.

(4) Hagfeldt, A.; Boschloo, G.; Sun, L.; Kloo, L.; Pettersson, H. Dye-Sensitized Solar Cells. *Chem. Rev.* **2010**, *110*, 6595−6663.

(5) Hashmi, G.; Miettunen, K.; Peltola, T.; Halme, J.; Asghar, I.; Aitola, K.; Toivola, M.; Lund, P. Review of Materials and Manufacturing Options for Large Area Flexible Dye Solar Cells. *Renewable Sustainable Energy Rev.* **2011**, *15*, 3717−3732.

(6) Pagliaro, M.; Ciriminna, R.; Palmisano, G. Flexible Solar Cells. *ChemSusChem* **2008**, *1*, 880−891.

(7) Chen, T.; Qiu, L. B.; Cai, Z. B.; Gong, F.; Yang, Z. B.; Wang, Z. S.; Peng, H. S. Intertwined Aligned Carbon Nanotube Fiber Based Dye-Sensitized Solar Cells. *Nano Lett.* **2012**, *12*, 2568−2572.

(8) Yin, X.; Xue, Z. S.; Wang, L.; Cheng, Y. M.; Liu, B. High-Performance Plastic Dye-Sensitized Solar Cells Based on Low-Cost Commercial P25 TiO_2 and Organic Dye. *ACS Appl. Mater. Interfaces* **2012**, *4*, 1709−1715.

(9) Yamaguchi, T.; Tobe, N.; Matsumoto, D.; Nagai, T.; Arakawa, H. Highly Efficient Plastic-Substrate Dye-Sensitized Solar Cells with Validated Conversion Efficiency of 7.6%. *Sol. Energy Mater. Sol. Cells* **2010**, *94*, 812−816.

(10) Yamaguchi, T.; Tobe, N.; Matsumoto, D.; Arakawa, H. Highly Efficient Plastic Substrate Dye-Sensitized Solar Cells Using a Compression Method for Preparation of TiO_2 Photoelectrodes. *Chem. Commun.* **2007**, 4767−4769.

(11) Zhang, D. S.; Yoshida, T.; Oekermann, T.; Furuta, K.; Minoura, H. Room-Temperature Synthesis of Porous Nanoparticulate TiO_2 Films for Flexible Dye-Sensitized Solar Cells. *Adv. Funct. Mater.* **2006**, *16*, 1228−1234.

(12) Park, N. G.; Kim, K. M.; Kang, M. G.; Ryu, K. S.; Chang, S. H.; Shin, Y. J. Chemical Sintering of Nanoparticles: A Methodology for Low-Temperature Fabrication of Dye-Sensitized TiO_2 Films. *Adv. Mater.* **2005**, *17*, 2349−2353.

(13) Zardetto, V.; Di Giacomo, F.; Garcia-Alonso, D.; Keuning, W.; Creatore, M.; Mazzuca, C.; Reale, A.; Di Carlo, A.; Brown, T. M. Fully Plastic Dye Solar Cell Devices by Low-Temperature UV-Irradiation of Both the Mesoporous TiO_2 Photo- and Platinized Counter-Electrodes. *Adv. Energy Mater.* **2013**, *3*, 1292−1298.

(14) Ito, S.; Ha, N. L. C.; Rothenberger, G.; Liska, P.; Comte, P.; Zakeeruddin, S. M.; Pechy, P.; Nazeeruddin, M. K.; Grätzel, M. High-Efficiency (7.2%) Flexible Dye-Sensitized Solar Cells with Ti-Metal Substrate for Nanocrystalline-TiO_2 Photoanode. *Chem. Commun.* **2006**, 4004−4006.

(15) Vomiero, A.; Galstyan, V.; Braga, A.; Concina, I.; Brisotto, M.; Bontempi, E.; Sberveglieri, G. Flexible Dye Sensitized Solar Cells Using TiO_2 Nanotubes. *Energy Environ. Sci.* **2011**, *4*, 3408−3413.

(16) Kuang, D.; Brillet, J.; Chen, P.; Takata, M.; Uchida, S.; Miura, H.; Sumioka, K.; Zakeeruddin, S. M.; Grätzel, M. Application of Highly Ordered TiO_2 Nanotube Arrays in Flexible Dye-Sensitized Solar Cells. *ACS Nano* **2008**, *2*, 1113−1116.

(17) Dürr, M.; Schmid, A.; Obermaier, M.; Rosselli, S.; Yasuda, A.; Nelles, G. Low-Temperature Fabrication of Dye-Sensitized Solar Cells by Transfer of Composite Porous Layers. *Nat. Mater.* **2005**, *4*, 607−611.

(18) Huang, X. M.; Huang, S. Q.; Zhang, Q. X.; Guo, X. Z.; Li, D. M.; Luo, Y. H.; Shen, Q.; Toyoda, T.; Meng, Q. B. A Flexible Photoelectrode for CdS/CdSe Quantum Dot-Sensitized Solar Cells (QDSSCs). *Chem. Commun.* **2011**, *47*, 2664−2666.

(19) Yang, L.; Wu, L.; Wu, M.; Xin, G.; Lin, H.; Ma, T. High-Efficiency Flexible Dye-Sensitized Solar Cells Fabricated by A Novel Friction-Transfer Technique. *Electrochem. Commun.* **2010**, *12*, 1000−1003.

(20) Wang, Z. R.; Wang, H.; Liu, B.; Qiu, W. Z.; Zhang, J.; Ran, S. H.; Huang, H. T.; Xu, J.; Han, H. W.; Chen, D.; Shen, G. Z. Transferable and Flexible Nanorod-Assembled TiO_2 Cloths for Dye-Sensitized Solar Cells, Photodetectors, and Photocatalysts. *ACS Nano* **2011**, *5*, 8412−8419.

(21) Fong, H. In *Polymeric Nanostructures and Their Applications*; Nalwa, H. S., Ed.; American Scientific Publishers: Stevenson Ranch, CA, 2007; Vol. 2, pp 451−474.

(22) Joshi, P.; Zhang, L.; Davoux, D.; Zhu, Z.; Galipeau, D.; Fong, H.; Qiao, Q. Composite of TiO_2 Nanofibers and Nanoparticles for Dye-Sensitized Solar Cells with Significantly Improved Efficiency. *Energy Environ. Sci.* **2010**, *3*, 1507−1510.

(23) Wang, X.; Karanjit, S.; Zhang, L.; Fong, H.; Qiao, Q.; Zhu, Z. Transient Photocurrent and Photovoltage Studies on Charge Transport in Dye-Sensitized Solar Cells Made from the Composites of TiO_2 Nanofibers and Nanoparticles. *Appl. Phys. Lett.* **2011**, *98*, 082114.

(24) Wang, X.; He, G.; Fong, H.; Zhu, Z. Electron Transport and Recombination in Photoanode of Electrospun TiO_2 Nanotubes for Dye-Sensitized Solar Cells. *J. Phys. Chem. C* **2013**, *117*, 1641−1646.

(25) Ye, M.; Xin, X.; Lin, C.; Lin, Z. High Efficiency Dye-Sensitized Solar Cells Based on Hierarchically Structured Nanotubes. *Nano Lett.* **2011**, *11*, 3214−3220.

(26) Ye, M.; Zheng, D.; Lv, M.; Chen, C.; Lin, C.; Lin, Z. Hierarchically Structured Nanotubes for Highly Efficient Dye-Sensitized Solar Cells. *Adv. Mater.* **2013**, *25*, 3039−3044.

(27) Wang, J.; Lin, Z. Q. Dye-Sensitized TiO_2 Nanotube Solar Cells with Markedly Enhanced Performance via Rational Surface Engineering. *Chem. Mater.* **2010**, *22*, 579−584.

(28) Xin, X. K.; Wang, J.; Han, W.; Ye, M. D.; Lin, Z. Q. Dye-Sensitized Solar Cells Based on a Nanoparticle/Nanotube Bilayer Structure and Their Equivalent Circuit Analysis. *Nanoscale* **2012**, *4*, 964−969.

(29) Hwang, D.; Jo, S. M.; Kim, D. Y.; Armel, V.; MacFarlane, D. R.; Jang, S.-Y. High-Efficiency, Solid-State, Dye-Sensitized Solar Cells Using Hierarchically Structured TiO_2 Nanofibers. *ACS Appl. Mater. Interfaces* **2011**, *3*, 1521−1527.

(30) Yang, S.; Zhu, P.; Nair, A. S.; Ramakrishna, S. Rice Grain-Shaped TiO_2 Mesostructures − Synthesis, Characterization and Applications in Dye-Sensitized Solar Cells and Photocatalysis. *J. Mater. Chem.* **2011**, *21*, 6541−6548.

(31) Poudel, P.; Qiao, Q. One Dimensional Nanostructure/Nanoparticle Composites as Photoanodes for Dye-Sensitized Solar Cells. *Nanoscale* **2012**, *4*, 2826−2838.

(32) Li, Y.; Lee, D. K.; Kim, J. Y.; Kim, B.; Park, N. G.; Kim, K.; Shin, J. H.; Choi, I. S.; Ko, M. J. Highly Durable and Flexible Dye-Sensitized Solar Cells Fabricated on Plastic Substrates: PVDF-Nanofiber-Reinforced TiO_2 Photoelectrodes. *Energy Environ. Sci.* **2012**, *5*, 8950−8957.

(33) Xi, M.; Wang, X. X.; Zhao, Y.; Feng, Q.; Zheng, F.; Zhu, Z.; Fong, H. Mechanically Flexible Hybrid Mat Consisting of TiO_2 and SiO_2 Nanofibers Electrospun via Dual Spinnerets for Photo-Detector. *Mater. Lett.* **2014**, *120*, 219−223.

(34) Li, Y.; Lee, W.; Lee, D. K.; Kim, K.; Park, N. G.; Ko, M. J. Pure Anatase TiO_2 "Nanoglue": An Inorganic Binding Agent to Improve Nanoparticle Interconnections in the Low-Temperature Sintering of Dye-Sensitized Solar Cells. *Appl. Phys. Lett.* **2011**, *98*, 103301−103304.

(35) Chandrasekar, R.; Zhang, L.; Howe, J. Y.; Hedin, N. E.; Zhang, Y.; Fong, H. Fabrication and Characterization of Electrospun Titania Nanofibers. *J. Mater. Sci.* **2009**, *44*, 1198−1205.

(36) Wen, S. P.; Liu, L.; Zhang, L. F.; Chen, Q.; Zhang, L. Q.; Fong, H. Hierarchical Electrospun SiO_2 Nanofibers Containing SiO_2 Nanoparticles with Controllable Surface-Roughness and/or Porosity. *Mater. Lett.* **2010**, *64*, 1517−1520.

(37) Zhu, K.; Neale, N. R.; Miedaner, A.; Frank, A. J. Enhanced Charge-Collection Efficiencies and Light Scattering in Dye-Sensitized

Solar Cells Using Oriented TiO$_2$ Nanotubes Arrays. *Nano Lett.* **2007**, *7*, 69−74.

(38) Frank, A. J.; Kopidakis, N.; van de Lagemaat, J. Electrons in Nanostructured TiO$_2$ Solar Cells: Transport, Recombination and Photovoltaic Properties. *Coord. Chem. Rev.* **2004**, *248*, 1165−1179.

(39) Neale, N. R.; Kopidakis, N.; van de Lagemaat, J.; Grätzel, M.; Frank, A. J. Effect of a Coadsorbent on the Performance of Dye-Sensitized TiO$_2$ Solar Cells: Shielding versus Band-Edge Movement. *J. Phys. Chem. B* **2005**, *109*, 23183−23189.

(40) Mohammadpour, R.; Iraji zad, A.; Hagfeldt, A.; Boschloo, G. Investigation on the Dynamics of Electron Transport and Recombination in TiO$_2$ Nanotube/Nanoparticle Composite Electrodes for Dye-Sensitized Solar Cells. *Phys. Chem. Chem. Phys.* **2011**, *13*, 21487−21491.

(41) Gao, R.; Tian, J.; Liang, Z.; Zhang, Q.; Wang, L.; Cao, G. Nanorod−Nanosheet Hierarchically Structured ZnO Crystals on Zinc Foil as Flexible Photoanodes for Dye-Sensitized Solar Cells. *Nanoscale* **2013**, *5*, 1894−1901.

(42) Barbé, C. J.; Arendse, F.; Comte, P.; Jirousek, M.; Lenzmann, F.; Shklover, V.; Grätzel, M. Nanocrystalline Titanium Oxide Electrodes for Photovoltaic Applications. *J. Am. Ceram. Soc.* **1997**, *80*, 3157−3171.

(43) Brown, T. M.; De Rossi, F.; Di Giacomo, F.; Mincuzzi, G.; Zardetto, V.; Reale, A.; Di Carlo, A. Progress in Flexible Dye Solar Cell Materials, Processes and Devices. *J. Mater. Chem. A* **2014**, *2*, 10788−10817.

(44) Hagendorfer, H.; Lienau, K.; Nishiwaki, S.; Fella, C. M.; Kranz, L.; Uhl, A. R.; Jaeger, D.; Luo, L.; Gretener, C.; Buecheler, S.; Romanyuk, Y. E.; Tiwari, A. N. Highly Transparent and Conductive ZnO:Al Thin Films from A Low Temperature Aqueous Solution Approach. *Adv. Mater.* **2014**, *26*, 632−636.

(45) Liu, X. Z.; Wang, L.; Xue, Z. S.; Liu, B. Efficient Flexible Dye-Sensitized Solar Cells Fabricated by Transferring Photoanode with a Buffer Layer. *RSC Adv.* **2012**, *2*, 6393−6396.